

SINGLE PARTICLE INCLUSIVE SPECTRA, HBT AND ELLIPTIC FLOW; A CONSISTENT PICTURE AT RHIC?

RAIMOND SNELLINGS
FOR THE STAR COLLABORATION

Lawrence Berkeley National Lab., 1 Cyclotron Rd, Berkeley, CA 94720, USA
E-mail: RJSnellings@lbl.gov

In these proceedings we will present the preliminary identified single particle inclusive spectra, the identified particle elliptic flow and the HBT versus the reaction plane measured with the STAR detector at RHIC. So far none of the theoretical space-time models has been able to describe the combination of these measurements consistently. In order to see if our measurements can be understood in the context of a simple hydro-motivated blast wave model we extract the relevant parameters for this model, and show that it leads to a consistent description of these observables.

1 Introduction

The goals of the ultra-relativistic nuclear collision program are the creation and detection of a system of deconfined quarks and gluons. Generally, one is interested in the bulk properties of this created system. Therefore one is interested in measuring the distribution of the produced particles both in momentum space and coordinate space. One year after the start of the RHIC program already a large amount of data has become available which addresses both momentum and coordinate space. Before this data became available a number of theoretical models with very different underlying assumptions were being considered. The constraints due to the measurements of the single particle inclusive spectra, the identified particle elliptic flow and HBT already show that none of the available “realistic” models is able to provide a complete picture of the underlying physics at RHIC. In the next three sections we will parameterize the single particle inclusive spectra, identified particle elliptic flow and HBT versus the reaction plane with a hydro-motivated blast wave model. Comparing the extracted parameters of these three different observables will determine if a description of the measurements with boosted thermal particle distributions (blast wave model) is warranted.

2 single particle inclusive spectra

The single hadron inclusive spectra reflect the freeze-out conditions of the system created in a heavy-ion collision. If the system interacted strongly

before freeze-out then the direct information of the interesting early collision stage is lost. This means that the single hadron inclusive spectra can only provide indirect information about the early collision stage.

Furthermore, if the system interacted strongly (due to rescattering) then the system could reach local thermal equilibrium. These rescatterings result in a pressure which causes the system to expand collectively. If all the particles freeze-out simultaneously and the system is in local thermal equilibrium their momentum spectra can be characterized by only two parameters, the temperature and the transverse collective flow velocity. The equation used to fit the spectra is described in Ref. ¹, the equation is based on boosted thermal particle distributions for an infinitely long solid cylinder (named blast wave model in these proceedings ²).

Fig. 1 shows the $m_t - m_0$ particle spectra for the negative pions, negative kaons, antiprotons and antilambdas measured in STAR. The figure shows that the m_t spectra can be characterized by the assumption of one average freeze-out temperature and one average transverse flow velocity for all particles. The values which are extracted, using a 63.8% confidence level, for the parameters are; $T = 120_{-25}^{+50}$ MeV and $\langle\beta_r\rangle = 0.52_{-0.08}^{+0.12} c$. It should be

noted that these spectra are preliminary and not corrected for feed-down and resonance contributions. The spectrum shapes clearly change as a function of the mass of the particle, which is what one would expect for boosted thermal spectra. However, the assumption of strong rescattering leading to transverse flow is not the only interpretation of the m_t dependence ^{3,4,5}. One explana-

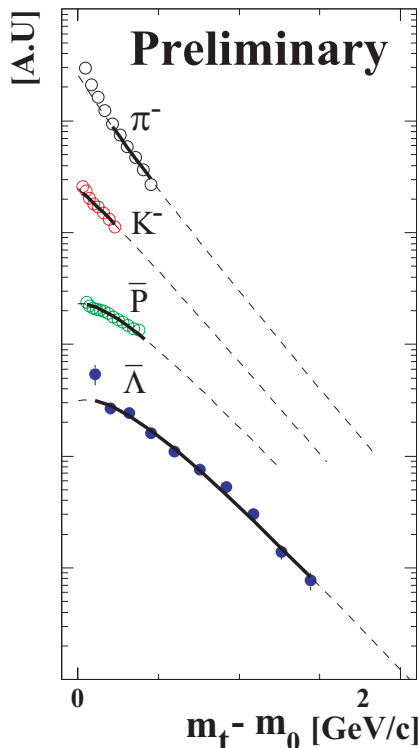


Figure 1. the m_t spectra for π^- , K^- , \bar{p} and $\bar{\Lambda}$ for the 6% most central events. The dotted lines show the fit with the blast wave model, and the solid lines show the region included in the fit. The scale of the ordinate is in arbitrary units.

tion of the observed spectrum shape could be that the particles are initially produced according to a thermal distribution. In this interpretation there is no transverse flow velocity. In the next section we will discuss the identified particle elliptic flow measurements. Elliptic flow is determined using two or higher order particle correlations^{6,7} and is therefore considered to be sensitive to the degree of collectivity of the observed particles and can help to resolve this ambiguity⁸.

3 Elliptic flow

The azimuthal anisotropy of the transverse momentum distribution of hadrons for non-central collisions also reflects the freeze-out conditions of the system created in heavy-ion collisions. The anisotropy is sensitive to the rescattering of the constituents in the created hot and dense matter. The second Fourier coefficient of this anisotropy, v_2 , is called elliptic flow.

Similar to the single particle inclusive spectra it does not provide direct (*i.e.* model independent) information about the early collision stage. However, the rescattering converts the initial spatial anisotropy, due to the almond shape of the overlap region of non-central collisions, into momentum anisotropy. The spatial anisotropy is largest early in the evolution of the collision, but as the system expands and becomes more spherical this driving force quenches itself. Therefore, in this picture, the magnitude of the observed elliptic

flow should reflect the extent of the rescattering at relatively early time⁹ and provides valuable indirect information about the early collision stage.

The first elliptic flow results from RHIC were for charged particles. The differential charged particle flow, $v_2(p_t)$, shows an almost linear rise with transverse momentum, p_t , up to 1.5 GeV/c. At $p_t > 1.5$ GeV/c, the

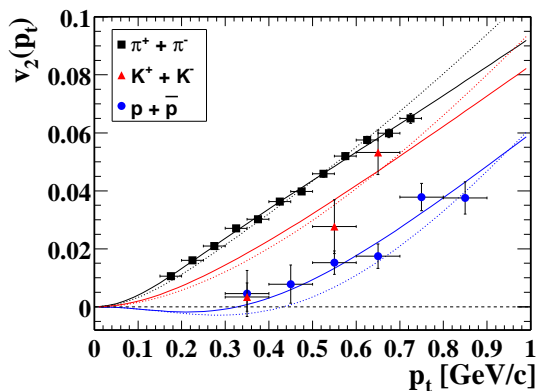


Figure 2. Differential elliptic flow for pions, kaons and protons + antiprotons for minimum-bias events. The solid lines show the fit with the modified blast wave model (including an elliptic deformation of the source), and the dotted lines are the fit with the unmodified model.

$v_2(p_t)$ values start to saturate, which might indicate the onset of hard processes^{10,11,12,13}. The behavior of $v_2(p_t)$ up to 1.5 GeV/ c is consistent with a hydrodynamic picture. Studies of the mass dependences of elliptic flow for particles with $p_t < 1.5$ GeV/ c provide important additional tests of the hydrodynamical model¹⁴. Similar to the identified single particle spectra, where the transverse flow velocity can be extracted from the mass dependence of the slope parameter, the $v_2(p_t)$ for different mass particles allows the extraction of the elliptic component of the transverse flow velocity^{15,16}. Moreover, the details of the dependence of elliptic flow on particle mass and transverse momentum are sensitive to the temperature, transverse flow velocity, its azimuthal variation, and source deformation at freeze-out.

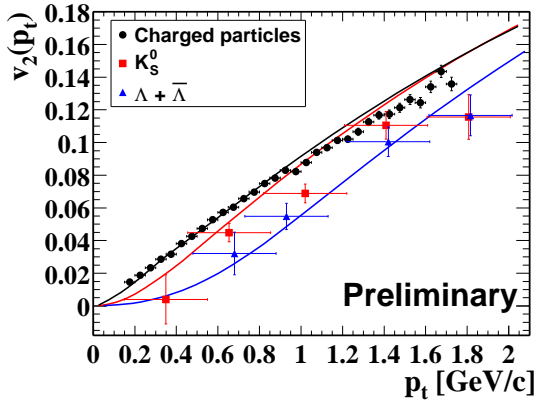


Figure 3. Differential elliptic flow for charged particles, K_S^0 and Λ s. The lines are the hydro model predictions for these particles.

In the region of overlapping p_t the K_S^0 v_2 agrees with the values for the charged kaons and for $\Lambda + \bar{\Lambda}$ the v_2 agrees with the protons + antiprotons v_2 . However, the statistical uncertainties are significant for the year-1 data which makes a detailed comparison impossible.

We have fitted the $v_2(p_t, m)$ data from Fig. 2 with a simple hydrodynamic-motivated model¹⁷. This model is a generalization of the blast wave model from^{2,14} assuming the flow field is perpendicular to the freeze-out hypersurface¹⁷. From this fit we have extracted the values for the average temperature (T), average transverse flow velocity (β_r), the average azimuthal variation of this transverse flow velocity (β_a) and the average elliptic deformation (s_2). Excluding the elliptic deformation of the source the extracted

The differential elliptic flow, v_2 , depends on mass, rapidity (y) and p_t . In Fig. 2, $v_2(p_t)$ is shown for pions, kaons, and protons + antiprotons for minimum-bias collisions, integrated over rapidity and centrality by taking the multiplicity-weighted average¹⁷. The behavior of $v_2(p_t)$ for pions, charged kaons and protons + antiprotons is fairly well described within a hydrodynamic model description¹⁴.

Fig. 3 shows the $v_2(p_t)$ for K_S^0 and $\Lambda + \bar{\Lambda}$ together with the charged particles.

parameters are; $T = 135 \pm 19$ MeV, $\beta_r = 0.52 \pm 0.03$ c and $\beta_a = 0.09 \pm 0.02$ c . However, the dotted lines showing the resulting fit in Fig. 2 do not provide an adequate description of the data. The fit including the elliptic deformation of the source, shown as full lines in Fig. 2, clearly describes the details of the $v_2(p_t, m)$. The extracted parameters with the elliptic deformation included are; $T = 101 \pm 24$ MeV, $\beta_r = 0.54 \pm 0.03$ c , $\beta_a = 0.04 \pm 0.01$ c and $s_2 = 0.04 \pm 0.01$.

Elliptic flow measurements characterize the second harmonic oscillation of the particle yield as a function of ϕ (where ϕ is the azimuthal angle versus the reaction plane), p_t and mass. This does not give us direct information about the source shape. From the fit to the data we infer that there are more emitted particles boosted in the direction of the reaction plane. This can be naturally explained by an elliptic deformation of the source. However, this is not the only explanation, a density modulation of sources as a function of ϕ would result in the same observed $v_2(p_t, m)$. This ambiguity can be resolved by looking at Hanbury-Brown and Twiss (HBT) interferometry versus the reaction plane.

4 HBT radii versus the reaction plane

Correlations between identical bosons at a given momentum probe the coordinate-space homogeneity lengths at that momentum. The homogeneity lengths (the HBT radii), e.g. defined parallel or perpendicular to the pair momentum, are the length scales characterizing the variance of particle positions emitted with a certain momentum. In the case of no space-momentum correlation (due to, for example, collective flow) the measurements would provide direct access to the freeze-out geometry. The single particle inclusive spectra and the $v_2(m, p_t)$ measurements can both be described under the assumption of strong collective flow. This would indicate the presence of strong space-momentum correlations, which will affect the observed HBT radii. Using the blast wave model to fit the HBT radii leads to a natural inclusion of the space-momentum correlations and allows us to compare to the parameters obtained from the single particle inclusive spectra and $v_2(m, p_t)$. A precise description of the implementation of the blast wave for the HBT measurement and a comparison of all the HBT radii is outside the scope of these proceedings but can be found in Ref ¹⁸. Here we will focus on the HBT radii relative to the orientation of the reaction plane. A theoretical description of the analysis technique is presented in ¹⁹. From the measured $v_2(p_t, m)$, we extracted the temperature, transverse flow velocity and the azimuthal variation of the transverse flow velocity. In addition this measurement indicates that there are

more particles boosted in the direction of the reaction plane than perpendicular to the reaction plane. This could be naturally explained by an extended source in the direction perpendicular to the reaction plane at freeze-out or by a larger source density in the reaction plane. These two scenarios would lead to an opposite oscillation of the HBT radii versus the reaction plane.

Fig. 4 shows R_o^2 , R_s^2 and R_{os}^2 as a function of the reaction plane angle. The solid lines show the expected oscillation when using the parameters obtained from fitting the $v_2(m, p_t)$. The observed HBT radii are in qualitative agreement with the expectation from these parameters. In addition the sign of the oscillation indicates that the source is extended perpendicular to the reaction plane. This analysis has been performed for Au+Au collisions at 2 – 6A GeV by E895²⁰ at the AGS. For the transverse radii they also concluded that the source revealed an “almond” transverse profile which had the longer axis perpendicular to the reaction plane.

Similar to the single particle inclusive spectra and $v_2(p_t, m)$, the HBT radii do not provide direct information about the early collision stage. However, in the case of strong elliptic flow the initial almond will grow faster along its shorter than its longer axis. This leads to the quenching of the driving force for elliptic flow but also to a more spherical source at freeze-out. Assuming that HBT measures the radii of homogeneity at thermal freeze-out, then the eccentricity of the source can be extracted with azimuthally sensitive HBT. However, even in the case of only strong transverse expansion both the radius in x and y will grow which will also lead to a smaller relative difference. Fig. 5 shows the ratio of the extracted RMS of y/x as a function of $\sqrt{s_{nn}}$. At the AGS energies the source deformation is still rather close to what one would expect from the initial deformation of the overlap geometry. At $\sqrt{s_{nn}} = 130$ GeV the system is apparently al-

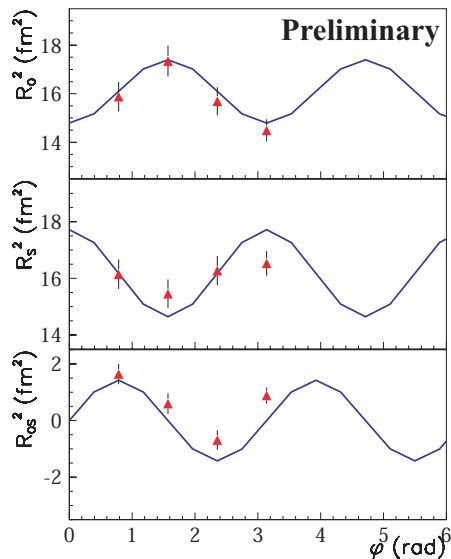


Figure 4. The azimuthal variation of R_o^2 , R_s^2 and R_{os}^2 . All three homogeneity lengths show a definite oscillation with respect to the reaction plane angle. The solid lines show the expected oscillation when using the parameters obtained from fitting the $v_2(m, p_t)$.

most spherically symmetric. This observation is consistent with a stronger collective expansion at RHIC before the particles freeze-out.

5 Conclusions

We have presented the single particle inclusive spectra for negative pions, negative kaons, antiprotons and antilambdas which can be characterized by two parameters, *i.e.* the temperature and the transverse flow velocity. We have shown that v_2 as a function of transverse momentum and mass can be characterized by the same two parameters with in addition, for these non-central collisions, an azimuthal oscillation of the transverse flow velocity and an elliptic deformation in

the transverse plane of the source. The elliptical deformation of the source can also be extracted from HBT measurements versus the reaction plane. We have shown that those three different observables lead to parameters in the context of a hydro motivated model which are in qualitative agreement with each other. However, one has to keep in mind that the blast wave fits to the different observables have not been done using exactly the same prescription. For $v_2(p_{t,m})$ the parameters were extracted using boosted thermal particle distributions on a thin shell (delta function) while for the single particle inclusive spectra and the HBT radii a solid cylinder with a flow profile ($\propto (r/R)^\alpha$) was used. The mean values of these parameters can be related to each other, however “small” differences due to the flow profile are lost. In the near future we will use the same prescription and constrain the parameters by a combined fit of the observables.

The qualitative agreement of the blast wave description with the three observables leads to the interpretation that for Au+Au collisions at $\sqrt{s_{nn}} = 130$ GeV the system can be characterized by boosted thermal particle distribu-

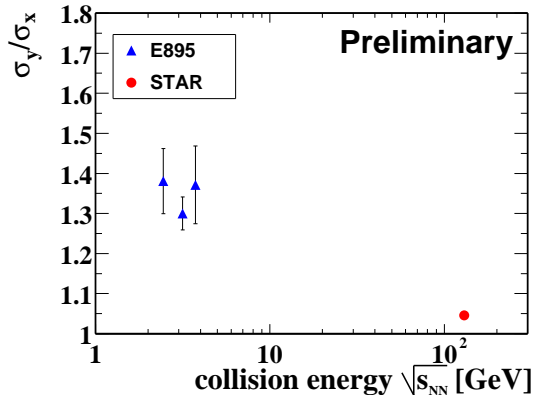


Figure 5. The ratio of the source variance in y and x . The triangles are the E895 measurements for Au+Au collisions at 2 – 6A GeV and the filled circle represents the STAR measurement at $\sqrt{s_{nn}} = 130$ GeV.

tions. This indicates strong space momentum correlations due to rescattering of the constituents. However, this blast wave parameterization does not give us any information about the initial conditions of the collision and does not tell us how and when the system reached this apparent boosted thermal behavior. This information could be extracted from more realistic models. However at this moment there are no models which give a microscopic and detailed time evolution of the system and are able to describe the combination of the single particle inclusive spectra, $v_2(p_{t,m})$ and HBT. Experimentally, measuring elliptic flow of particles with small hadronic cross-sections (like the Φ meson) would provide us with more model independent information about when the system reached this boosted thermal behavior.

Acknowledgments

We wish to thank the RHIC Operations Group and the RHIC Computing Facility at Brookhaven National Laboratory, and the National Energy Research Scientific Computing Center at Lawrence Berkeley National Laboratory for their support. This work was supported by the Division of Nuclear Physics and the Division of High Energy Physics of the Office of Science of the U.S. Department of Energy, the United States National Science Foundation, the Bundesministerium fuer Bildung und Forschung of Germany, the Institut National de la Physique Nucleaire et de la Physique des Particules of France, the United Kingdom Engineering and Physical Sciences Research Council, Fundacao de Amparo a Pesquisa do Estado de Sao Paulo, Brazil, the Russian Ministry of Science and Technology and the Ministry of Education of China and the National Science Foundation of China.

References

1. E. Schnedermann, J. Sollfrank and U. Heinz, Phys. Rev. C **48** 2462 (1993).
2. P. Siemens and J.O. Rasmussen, Phys. Rev. Lett. **42**, 880 (1979).
3. A. Leonidov, M. Nardi and H. Satz, Z. Phys. C **74**, 535 (1997).
4. L. McLerran and J. Schaffner-Bielich, Phys. Rev. B **514**, 29 (2001).
5. J. Schaffner-Bielich, D. Kharzeev, L. McLerran and R. Venugopalan, preprint nucl-th/0108048.
6. P. Danielewicz and G. Odyniec, Phys. Lett. B **157**, 146 (1985); A.M. Poskanzer and S.A. Voloshin, Phys. Rev. C **58**, 1671 (1998).
7. N. Borghini, P.M. Dinh and J.-Y. Ollitrault, Phys. Rev. C **63**, 054906 (2001); Phys. Rev. C **64**, 054901 (2001).

8. See also J-Y. Ollitrault, these proceedings.
9. H. Sorge, Phys. Lett. B **402**, 251 (1997).
10. STAR Collaboration, K.H. Ackermann *et al.*, Phys. Rev. Lett. **86**, 402 (2001).
11. X.N. Wang, Phys. Rev. C **63**, 054902 (2001).
12. M. Gyulassy, I. Vitev and X.N. Wang, Phys. Rev. Lett. **86**, 2537 (2001).
13. D. Molnár and M. Gyulassy, preprint nucl-th/0102031.
14. P. Huovinen, P.F. Kolb, U. Heinz, P.V. Ruuskanen and S. Voloshin, Phys. Lett. B **503**, 58 (2001).
15. EOS Collaboration, S. Wang *et al.*, Phys. Rev. Lett. **76**, 3911 (1996).
16. E877 Collaboration, S.A. Voloshin, Nucl. Phys. **A638**, 455c (1998).
17. STAR Collaboration, C. Adler *et al.*, Phys. Rev. Lett. **87**, 182301 (2001).
18. F. Retière, for the STAR Collaboration, preprint nucl-ex/0111013; M.A. Lisa, in preparation.
19. M.A. Lisa, U. Heinz and U.A. Wiedemann, Phys. Lett. B **489**, 287 (2000).
20. E895 Collaboration, M.A. Lisa *et al.*, Phys. Lett. B **496**, 1 (2000).